DESIGN PROCEDURE FOR A FOWLER FLAP MECHANISM

Gustavo Limongi Araújo
Instituto Tecnológico de Aeronáutica-ITA
gustavo.limongi@embraer.com.br

Sergio Frascino Müller de Almeida
Instituto Tecnológico de Aeronáutica-ITA
frascino@ita.br

Abstract. *Control Surfaces like flap are employed in the leading and trailing edges during some phases of the flight like landing, approach and take-off for lift augmentation. This work studies the flap control surface actuation mechanism to evaluate the influence of the clearances, dimensional and geometrical tolerances, tracks misalignment and the panel stiffness during its operation at the design phase. The purpose of this work is to develop an efficient and precise method for trade-off studies between the force exerted by the actuators and the tracks misalignment, clearances and system flexibility.*

Keywords*: flap, mechanism, tolerances, actuators, control surfaces, aeronautical engineering.*

1. Introduction

Flaps may be used to increase the maximum lift coefficient, increase the wing area, or both. A change in the maximum lift coefficient may be obtained by a change in the shape of the airfoil section or by increased camber. The trailing-edge flap is one method of accomplishing this. The maximum lift coefficient for an airfoil with a simple flap is greater than that for the unflapped airfoil. Also, the coefficients of lift are increased over the entire angle-of-attack range.

A Fowler flap can move back to increase the airplane wing area and may be rotated downward to increase the camber. A very large increase in maximum lift coefficient results. It may also be noted that flaps in an extreme down position (50° to 90°) act as a high-drag device and can retard the speed of an airplane before and after landing (de Andrade, 1999). A Fowler flap actuation mechanism is designed with redundant actuators to move a panel supported by rollers and tracks. There may be a misalignment due to the wing torsion when the flap is deployed during flight. If the panel has adequate flexibility and/or there are large clearances between rollers and tracks, the mechanism can accommodate the track misalignment without jamming. On the other hand, a flap designed to be very stiff and with minimum clearances will require high actuation forces during deployment. The purpose of this work is to propose a robust design procedure for control surfaces such as flaps and to study the effect of possible manufacturing interferences between rollers and tracks.

Since the flap movement is quasi-static the inertial forces may be neglected. A flap finite element model is developed to determinate the relation between the force exerted by the actuators and track misalignment without clearance. The panel stiffness matrix was obtained by using the stiffness influence coefficient method. A flap multibody model was also developed by using the LMS.Dads® software. The dimensional variation of flap components and tolerance assembly is performed by using the tolerance analysis and simulation software 3DCS CAA V5 based®. Considering the flap actuator has a limit force to operate, a design procedure is proposed to relate the actuator force to the flap stiffness and tracks misalignments. This procedure determines if the flap operates within an acceptable region, i.e., below the actuator limit force such as no jamming occurs.

2. Finite element model without clearance

The fowler flap considered in this work is composed of a single panel supported by four rollers into four fixed tracks. An arbitrary misalignment of the fourth roller with respect to the plane formed by the others three rollers was taken into account. This misalignment is due to the wing torsion during the take-off and landing and manufacturing / assembly tolerances. Moreover, during the flap assembly process in the wing, the airplane is sustained by jacks, so these tools produce torsion in the wing. Considering this situation the flap tracks are assembled with a relative misalignment between them. A flap panel finite element model was developed to determinate the relation between the actuator force and tracks misalignment assuming that there are no clearances between rollers and tracks.

Applying the virtual work principle, the virtual work exerted by the actuators is equal to the variation of the panel strain energy due to track misalignment,

$$\delta(\{u\}^T\{P\}) = \delta\left(\frac{1}{2}\{u\}^T[K]\{u\}\right). \tag{1}$$

Calculating the variations yields:

$$\{P\} = [K]\{U\}, \tag{2}$$

where $\{U\}$ is the rollers displacement vector in each time increment, $[K]$ is the panel stiffness matrix obtained from the influence coefficients and $\{P\}$ is the actuator force vector.

The procedure to determinate the stiffness influence coefficients consists in applying a unit prescribed displacement at point i and getting the reaction force at point j ($[K_{ij}]$ term). The panel has 6 points of interest known as attachment points (*Craig*, 1981), i.e., fixed points: 4 points related to the rollers (2 of each side) and more 2 points related to the actuator force application, as depicted in the Fig.1.

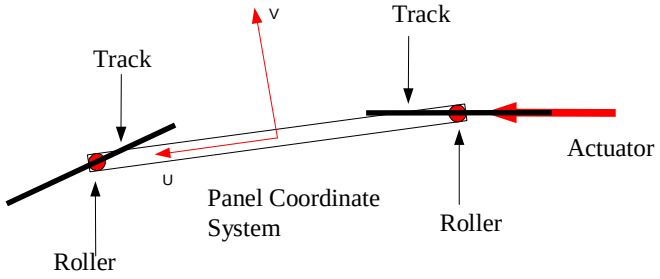

Fig.1. Mechanism geometry.

The flap panel was modeled with isoparametric shell elements (*Bathe*, 1996 and *Cook*, 1989) known as CQUAD4 (*John and John*, 1994). In order to obtain the stiffness matrix, 10 subcases were used related to the fixed points degrees of freedom (Fig.2).

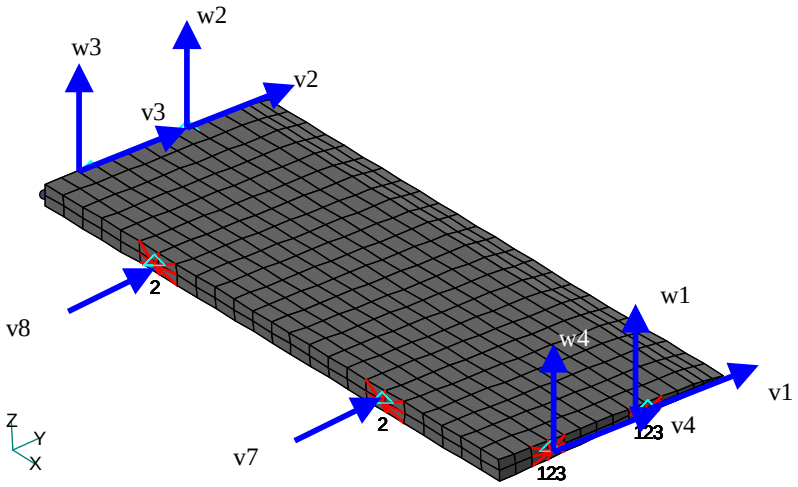

Fig.2. Panel finite element model and coordinate system <u, v, w>.

In the first subcase, correspondent to the first row of Tab.1, a unit prescribed displacement in the v_1 degree of freedom was applied. The obtained values are the reactions [kN/m] in the constraints related to the degrees of freedom showed in Fig.2. The panel stiffness matrix $[K]$ (Tab.1) was defined considering no misalignments. A misalignment is modeled as the rotation of the flap tracks. This rotation is obtained by pre- and post multiplying the stiffness matrix $[K]$ by the rotation matrix $[T]$ and its transpose. Matrix $[K']$ corresponding to rotating the track at node 1 (Fig.2) by an angle $\theta = 45°$, can be obtained from:

$$[K'] = [T]^t [K] [T], \tag{3}$$

where $[T]^t$ is the transpose rotation matrix and $[T]$ is the rotation matrix given by:

$$[T]=\begin{bmatrix} \cos(\theta) & 0 & 0 & 0 & sen(\theta) & 0 & 0 & 0 & 0 & 0 \\ 0 & 1 & 0 & 0 & 0 & 0 & 0 & 0 & 0 & 0 \\ 0 & 0 & 1 & 0 & 0 & 0 & 0 & 0 & 0 & 0 \\ 0 & 0 & 0 & 1 & 0 & 0 & 0 & 0 & 0 & 0 \\ -sen(\theta) & 0 & 0 & 0 & \cos(\theta) & 0 & 0 & 0 & 0 & 0 \\ 0 & 0 & 0 & 0 & 0 & 1 & 0 & 0 & 0 & 0 \\ 0 & 0 & 0 & 0 & 0 & 0 & 1 & 0 & 0 & 0 \\ 0 & 0 & 0 & 0 & 0 & 0 & 0 & 1 & 0 & 0 \\ 0 & 0 & 0 & 0 & 0 & 0 & 0 & 0 & 1 & 0 \\ 0 & 0 & 0 & 0 & 0 & 0 & 0 & 0 & 0 & 1 \end{bmatrix}, \tag{4}$$

Table 1. Stiffness matrix 10 x 10 (Influence Coefficients)

Stiffness matrix terms to the fixed points degrees of freedom. Unit:[kN/m]									
v_1	v_2	v_3	v_4	w_1	w_2	w_3	w_4	v_7	v_8
62925.2	599.5	616.3	-47041.4	0.7	-0.7	0.7	-0.7	-20152.3	3052.6
599.5	62923.7	-47043.5	616.4	0.2	-0.2	0.2	-0.2	3050.3	-20146.4
616.3	-47043.5	60353.1	559.3	0.5	-0.5	0.5	-0.5	1310.1	-15795.3
-47041.4	616.4	559.3	60349.9	0.3	-0.3	0.3	-0.3	-15793.0	1308.8
0.7	0.2	0.5	0.3	297.6	-297.6	297.6	-297.6	-0.8	-0.9
-0.7	-0.2	-0.5	-0.3	-297.6	297.6	-297.6	297.6	0.8	0.9
0.7	0.2	0.5	0.3	297.6	-297.6	297.6	-297.6	-0.8	-0.9
-0.7	-0.2	-0.5	-0.3	-297.6	297.6	-297.6	297.6	0.8	0.9
-20152.3	3050.3	1310.1	-15793.0	-0.8	0.8	-0.8	0.8	54160.2	-22575.3
3052.6	-20146.4	-15795.3	1308.8	-0.9	0.9	-0.9	0.9	-22575.3	54155.6

Applying the degrees of freedom condensation method *(Craig*, 1981) to matrix [*K*'], it can be rewritten as:

$$\begin{bmatrix} \{0_{4x1}\} \\ \{P_{6x1}\} \end{bmatrix} = \begin{bmatrix} [K_{uu(4x4)}] & [K_{up(4x6)}] \\ [K_{pu(6x4)}] & [K_{pp(6x6)}] \end{bmatrix} \begin{bmatrix} \{a_{u(4x1)}\} \\ \{a_{p(6x1)}\} \end{bmatrix} \tag{5}$$

where $\{a_p\}$ is the vector of the vertical displacements of the rollers (w_1, w_2, w_3, w_4) and the horizontal displacements of the attachment points of the actuators (v_7, v_8). Therefore,

$$\{P\} = \left([K_{pp}] - [K_{pu}][K_{pu}]^{-1}[K_{up}] \right) \{a_p\} \tag{6}$$

where $\{P\}$ is a vector containing the actuator forces required to move the panel for a misalignment of $\theta = 45°$ and the corresponding track vertical reactions. Considering an angle $\theta = 0°$ between the actuator and the panel and arbitrary displacement of 0.4m for each actuator, vector $\{a_p\}$ and the force vector $\{P\}$ are computed from Eq. (5); the results are given in Tab. 2.

The forces related to the degrees of freedom v_7 = 147.8 kN and v_8 = -30.1 kN correspond to the required actuator forces to move the panel by 0.4 m with a $\theta = 45°$ misalignment assumed at node 1. The forces associated to the *w* degrees of freedom correspond to the normal reaction forces applied by the rollers in the panel.

The values obtained by static condensation procedure were validated with a panel modeled in MSC.Nastran® simulating the forces and boundary conditions of the static condensation method described above. The correlations between the both methods are exact once the procedures are equivalent. From the stiffness matrix [*K*'] updated for each flap position during deployment it is possible to get the actuator force history required to move the panel with track misalignment. This problem has a linear solution; the solution is robust and fast. This same problem is modeled in section 3 by using multibody simulation software.

Table 2. Results obtained by Static Condensation

Degree of Freedom	$\{a_p\}$ [m]	$\{P\}$ Force [kN]
$w_{1'}$	0	-166.5
w_2	0	117.7
w_3	0	-117.7
w_4	0	117.7
v_7	0.4	147.8
v_8	0.4	-30.1

3. Multibody Model

A multibody model of the flap mechanism was created by using the LMS.Dads® (*Dynamic Analysis and Design System*), computational simulation tool widely used in the aerospace industry to analyze the dynamic behavior of mechanical system. Dads® is not a finite element package, but can be used together with FEA (Finite Element Analysis) to analyze the behavior of flexible components in the multibody model. This model, compared with the FEA model described in the previous section, is much more realistic as it includes joint definition between body parts, contact elements between rollers and tracks, aerodynamic load application and insertion of the flap panel finite element model. The main advantage of this multibody model compared to the FEA model is that clearance between roller and tracks may be added. The correlation between a linear static solution and dynamic solution is possible since the flap movement is quasi-static and the inertia forces may be disregarded. On the other hand the finite element model can be solved in much less time.

A multibody model is represented by a set of rigid and flexible bodies connected by joints (constraints) which are submitted to forces and prescribed displacements (drivers). Each rigid body uses a set of generalized coordinates to define the position and orientation of the body at each timestep. Three coordinates are used for the position of the mass center; typically, three coordinates are used to orient the body in space (Euler angles). Alternatively, four Euler parameters (*Shabana*, 1989) are used to define the body orientation (this option is used by DADS®). Therefore, each rigid body adds 6 degrees of freedom (u, v, w and ϕ, θ, Ψ) if Euler angles are used or 7 degrees of freedom if Euler parameters (u, v, w and e_0, e_1, e_2, e_3) are used to orient the body. Each joint constraints a number of degrees of freedom according to the joint type used. The formulation used to define the rigid body movement in the space is the Lagrange equations with constraints (*Meirovitch*, 1970).

3.1. Dads® Model Description

The fowler flap model developed in Dads® has 9 rigid bodies and 1 flexible body (panel) as showed in Fig. 3. The rigid bodies are the right and left actuators (divided into pre-actuator and actuator), rollers and fixed body. The flexible body is represented by the flap panel.

The system has redundant actuators to move the flap. In each actuator there is a spherical joint connecting the pre-actuator and ground (fixed body), a prismatic joint connecting the pre-actuator to the actuator and a revolute joint connecting the actuator to the flexible panel. The flexible panel, however, is fixed to 4 rigid rollers by a bracket joint, this joint constraints all degrees of freedom.

Contact elements type point-to-segment are used between the rollers that are geometrically defined as rigid spheres and the tracks that are geometrically defined as surfaces. In this kind of contact, the forces are generated between the point body (i.e., the rollers) and a surface in the segment body (i.e., the fixed body). The surface is formed by a track profile extrusion following the z-axis of the segment body triad. In this model a hertzian contact is taken into account. The hertzian contact force is function of several variables: material Young's module, materials restitution coefficient in contact and transition velocity etc. This contact works like a non-linear spring between 2 bodies.

3.2. Modeling of the flap panel flexibility

The flexible body modeling of the flap panel is essential to allow the modeling of track misalignment. The procedure to insert FEA models into multibody software is not trivial and follows a series of procedures and approaches described in this section. Dads® has a module for flexibility insertion named Dads/Flex®. This technique follows a method known as CMS, Component Mode Synthesis (*Craig*, 1981). In this approach, the body flexibility is represented by a set of dynamic and static modes; the latter type of modes are used to account for localized deformation effects.

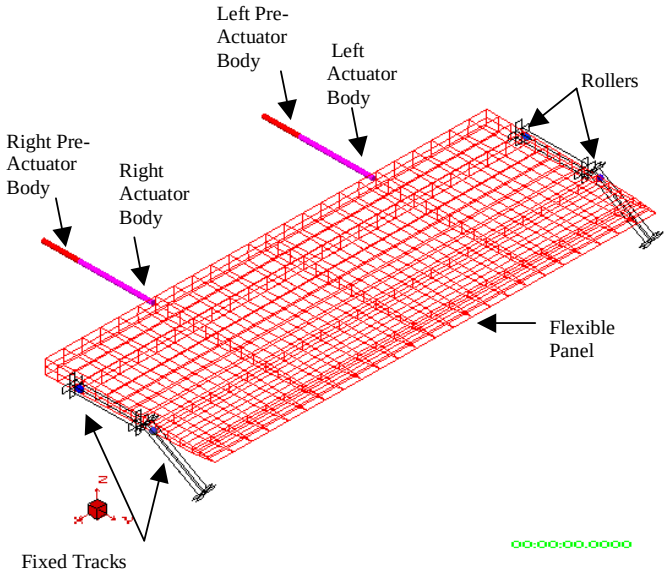

Fig.3. Multibody Model (isometric view).

The Craig-Bampton modes (*Craig and Bampton*, 1968) are a particular case of CMS. In the Craig-Bampton modes, the static modes are calculated considering the structure constrained at the attachment points in the degrees of freedom constrained by the joints. Therefore, the normal modes calculated by this method are called fixed interface normal modes. In addiction, a linear static solution is used to calculate the static modes in the interface nodes. The static modes are created by applying a unit prescribed displacement in each degree of freedom constrained by the joint. This kind of static mode is known as *static constrained mode* (*Craig*, 1981).

A careful selection of static modes should be done since the contribution of these modes to the system response is more important than the dynamic modes, since the flap movement is quasi-static.

Summarizing, the flexibility modeling in Dads® follows the steps described below:

1. To choose the rigid body will be replaced by the flexible one;
2. To use a finite element software (MSC.Nastran®) to create the body finite element mesh;
3. To calculate the normal modes with the same constraint the model is constrained by Dads®;
4. To calculate the static modes by applying a unit prescribed displacement in each degree of freedom constrained by the interface joints;
5. To generate the MSC.Nastran® files that will be inserted into DFBT (Dads Flexible Body Translator). The DFBT creates a file can be read by Dads/Flex®;
6. In Dads/Flex® a nodal reduction should be performed, keeping the attachment nodes in the model.
7. Into Dads/Flex® an orthogonalization should be performed to create a new mode set with modes linearly independent.
8. To update the joints applied in the flexible body.

Aerodynamic loads were applied at 4 discrete points normal to the panel surface localized between the reinforcements. This load is proportional to the flap deployment angle and it reaches the maximum value at the time step the flap deployment is maximum.

3.3. Results

The forces required to move the flap under an arbitrary aerodynamic load of 20000 N distributed into 4 discrete points were obtained assuming track misalignment. Two cases were considered: with clearance and without clearance between the rollers and tracks. The forces were obtained for the left actuator where the misalignment was applied. Results were obtained for 2 situations. Fig.4 presents the results without misalignment, and in Fig.5 the misalignment is 3°. The results in both plots were obtained without clearance between rollers and tracks and with a clearance of 0.27 mm.

The clearance does not affect the force required to move the panel when the tracks are perfectly aligned. On the other hand, when there is misalignment, the force to move the flap, under aerodynamic load, is sensible to the existence of clearance in the flap maximum deployment angle. Clearance causes the actuator force to decrease and is equivalent to misalign the tracks by a smaller angle.

Case 1 - Aligned tracks (with and without clearance).

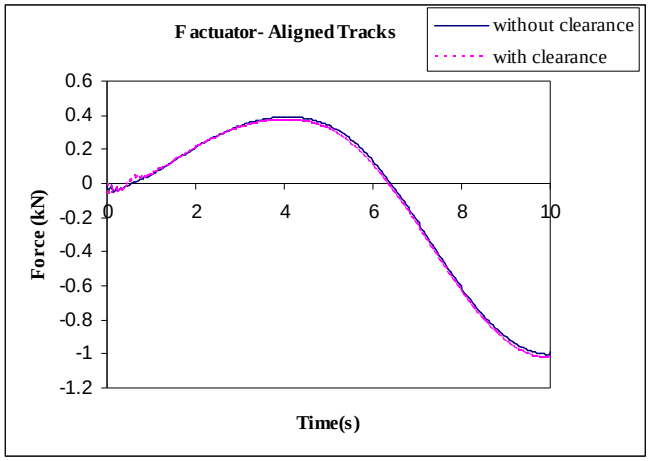

Fig.4. Aligned Tracks

Case 2 - Misaligned tracks -3 degrees (with and without clearance).

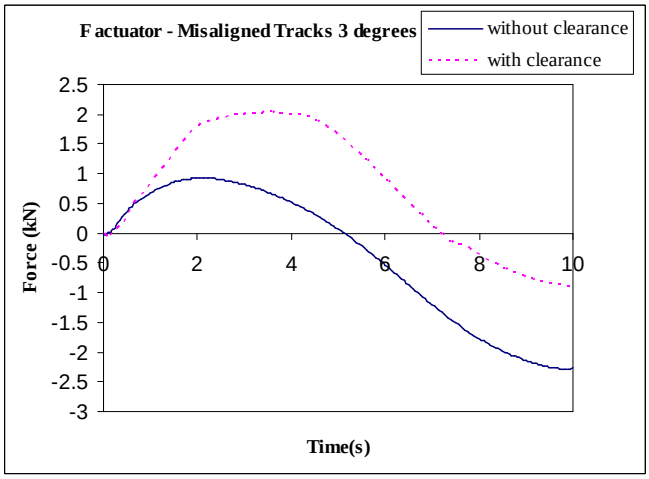

Fig.5. Misaligned Tracks

4. Tolerance Analysis

The performance of the flap actuation mechanism is affected by the assembly process of the system into the wing, by the primary components dimensional variation due to the assembly pretension, and a large number of dimensional factors that are subject to variation.

There are two fundamental tools to improve the tolerance specification. The first one is called GD&T (Geometric Dimensioning and Tolerancing), a language to apply tolerances into drawings sustained by three principles: tolerance application as a function of the product requirements; the use of a uniform language to express these tolerances aiming at minimizing the interpretation errors in the product loop; and in the normalization of this language as commercial relation guarantee between the companies, partners, suppliers and contractors. This GD&T normalization is based on ASME Y14.5M-1994. The second tool to improve the tolerance specification is the use of a computational package to aid in the product geometric specification. These systems have mathematical resources capable to identify and solve assembly errors and tolerance incompatibility by computational simulations during the design phase. These systems can determinate if the component tolerances will satisfy a statistical capacity level for the entire mechanical system (C_p and C_{pk}).

The software used for the dimensional and geometric tolerance analysis and simulation is the 3DCS® CAA (3-Dimensional Control System) CATIA V5 based. These programs simulate the assembly condition in the mechanical whole using the Monte Carlo (*Creveling*, 1997) algorithm. The tolerance simulation with 3DCS® for computing the tracks position tolerances includes the use of a false flap as an assembly resource tool (false flap is a tool with pegs that represents the minimum geometrical and dimensional variation). The holes are passed from one part to another reducing the dimensional variation in the complete system. In the flap assembly a false wing is also used as tooling. With this approach, the dimensional variations are reduced, but not completely eliminated.

The flap simulation results in a roller diameter to avoid assembly pretension that is smaller than the actual roller design diameter. Therefore, the system works with pretension even using tooling as resource. It is not possible to decrease this assembly interference even working with very small tolerances. A solution should be to increase the clearance between the roller and track. However, in order to minimize the problems due to the system transversal vibrations, the design clearance should be kept within (0.10-0.27 mm). The pretension calculated by 3DCS® is given by the roller minor diameter minus the roller diameter that always assemble. This value is equal to 0.7585 mm. It works as a pretension spring in the system that can work either for or against the flap movement.

5. Design Procedure

Since the inertial forces can be discarded, the correlation between the FEA model and the multibody model is possible. Disregarding the effect of clearance between roller and track, the FEA model has a good correlation with the multibody model. The finite element model is linear hence its solution is fast and the effect of structural stiffness may be studied simply by changing the material modulus of elasticity. The multibody model, however, is complex and the flexibility insertion task is not trivial. The solution time is much larger than that of the FEA model.

It is possible to relate the track misalignment, the panel stiffness variation and the actuator force through a plot that defines a range where the system operates properly, i.e., the required force to move the system is less than actuator maximum force. On the other hand, there is a region where the operation is unfeasible. The structure stress level was not taken into account to determinate the feasible region.

The correlation between the FEA and multibody model was performed for the flap maximum deployment angle (22°). Since the linear static solution does not consider the follower force effect, the boundary condition of the FEA model must be changed for each time step. These boundary conditions imply that the aerodynamic force should be normal to the panel surface for any deployment angle. This procedure is equivalent to put the deployed flap in an inclined plane with an incline angle equal to the control surface deflection angle.

The trade-off plot between track misalignment, panel stiffness and actuator force is showed in the Fig.6. These curves were obtained by using the FEA model with several track misalignment and panel stiffness combinations. The FEA model was run 121 times for each curve. The red curve, for example, represents the configurations (track misalignment and flap panel stiffness combinations) for which the left actuator has applied a maximum force of 3000 N to move the flap. Above the red curve the required force to move the flap is larger than the actuator maximum force; therefore, the system jams. On the other hand in the region below this curve the flap mechanism operates properly. These curves are not deterministic. The clearance existence between rollers and tracks changes the current values to a minor range as described in the item 3. For a given panel structural stiffness, it is possible to determinate what is the maximum allowable misalignment such that the flap may still be deployed by using Fig. 6. Also, if the maximum track misalignment is known, is possible to set the correct flap panel stiffness to keep the system in the feasible region.

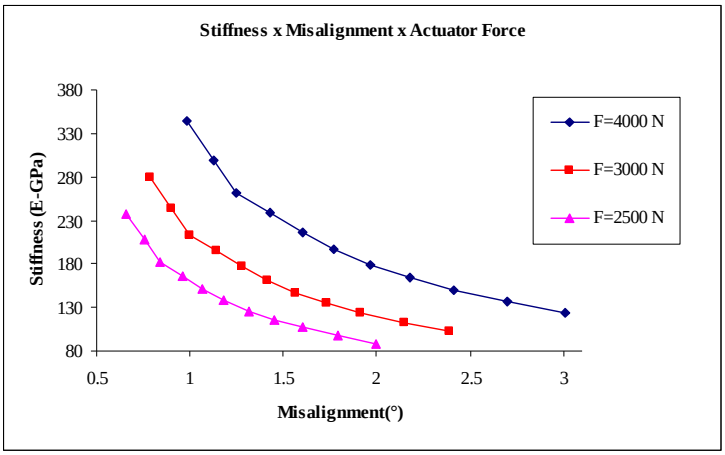

Fig.6. Design Procedure.

6. Conclusions

The flap design involves the trade-off analysis between track misalignment, flap panel stiffness and assembly pretension to move the system under aerodynamic load.

The multibody model has the advantage of including clearance between rollers and tracks; however it is complex and requires a high solution time compared to the FEA model that does not account for clearances. The clearances decrease the required forces to move the flap.

In order to minimize problems due to transverse vibration between rollers and tracks, the clearance between them should be very small. A judicious assembly rule is the use of appropriate tooling. In this case the assembly cycle is increased to break the tolerance loop in order to reduce the dimensional variation in the whole set. Even using this method the studied system will work with pretension.

There are some alternatives to overcome these problems:

- To increase the actuator force limit by specifying a system with more power; this alternative increases the system weight/cost relation;
- To increase the clearance between roller and track to minimize pretension assembly effects; this approach is limited due to transversal vibration such as *buffeting*;
- To tailor the panel stiffness; decreasing the flap stiffness may cause structural failure, buckling and/or aeroelasticity problems.

7. References

ASME, American Society for Mechanical Engineers, *"Dimensioning and Tolerancing ASME Y14.5M"*, New York, 1994.

BATHE, J. K., *Finite Element Procedures*, New Jersey, Prentice Hall, 1996.

COOK, R. D.; MALKUS, D. S.; PLESHA, M. E., *Concepts and applications of the finite element analysis*, New York , John Wiley, 1989.

CRAIG, R. R., *Structural Dynamics: An Introduction to Computer Methods*, John Wiley, 1981.

CRAIG, R. R.; BAMPTON, M. C. C., *"Coupling of Substructures for Dynamic Analyses"*, Washington, AIAA Journal, Vol.6, no.7, pages 1313-1319, 1968.

CREVELING, C. M., *Tolerance Design: A Handbook for Developing Optimal Specifications*, Rochester Institute of Technology, Prentice-Hall, , 1997.

DE ANDRADE, Donizeti, "*Notas de Aula Curso Fundamentos da Engenharia Aeronáutica*", ITA, São José dos Campos - SP, 1999.

JOHN, P. C.; JOHN, M. L., *MSC/Nastran® Linear Static Analysis*, Los Angeles, The Macneal-Schwendler, 1994.

MEIROVITCH, L., *Methods of analytical dynamics*, New York, McGraw-Hill, 1970.

MEIROVITCH, L., *Dynamics and control of structures*, New York, John Wiley & Sons, 1990.

SHABANA, A. A. *Dynamics of multibody systems*, New York, John Wiley & Sons, 1989.

8. Responsability notice

The authors are the only responsible for the printed material included in this paper.